

Variation in Charge-Transfer Photochemistry Clarified by a CASSCF/MR-CCI Comparative Study of the Low-Lying Excited States of $M(R)(CO)_3(H-DAB)$ ($M = Mn, R = H, \text{Methyl, Ethyl}; M = Re, R = H; DAB = 1,4\text{-Diaza-1,3-butadiene}$)

D. Guillaumont,[†] M. P. Wilms,[‡] C. Daniel,^{*,†} and D. J. Stufkens[‡]

Laboratoire de Chimie Quantique, UMR 7551 du CNRS et de l'Université Louis Pasteur, Institut Le Bel, 4 Rue Blaise Pascal, 67 000 Strasbourg, France, and Anorganisch Chemisch Laboratorium, Institute of Molecular Chemistry, Universitei van Amsterdam, Nieuwe Achtergracht 166, Amsterdam NL 1018WV, The Netherlands

Received March 6, 1998

The lowest energy electronic transitions of the model complexes $M(R)(CO)_3(H-DAB)$ ($M = Mn, R = H, CH_3, C_2H_5; M = Re, R = H, \alpha\text{-diimine} = H-DAB = 1,4\text{-diaza-1,3-butadiene}$) are investigated with the use of CASSCF/MR-CCI calculations. On the basis of the excitation energies calculated for the low-lying $nd \rightarrow \pi^*_{DAB}$ (metal-to-ligand-charge-transfer), $\sigma_{M-R} \rightarrow \pi^*_{DAB}$ (sigma-bond-to-ligand-charge-transfer), and $nd \rightarrow nd$ (metal-centered) excited states, it is shown how the three-center interaction between the R group, the metal center, and the π^* acceptor DAB ligand controls the nature and the energies of the lowest electronic transitions of these molecules. In the manganese hydride complex, the low-lying excited states are nearly pure, corresponding either to MLCT states in the visible energy domain between 15 090 and 26 000 cm^{-1} and 26 000 cm^{-1} or to SBLCT states calculated at 34 390 and 37 950 cm^{-1} for the triplet and for the singlet components, respectively. The calculated oscillator strengths indicate a large contribution of the second MLCT state, corresponding to the $3d_{xz} \rightarrow \pi^*_{DAB}$ excitation, to the intense visible band observed in this class of complexes. The transitions to the singlet and triplet MC excited states are calculated at 35 900 and 26 380 cm^{-1} , respectively, and will contribute to the UV absorption together with those to the SBLCT states. On going from the hydride to the methyl complex, the main change is a drastic lowering of the transition energies, which may exceed 0.5 eV for the SBLCT states. This effect is largely due to the weakening of the metal–R bond, the basicity of CH_3^- , and the more polarized character of the metal–methyl bond. On going from the methyl to the ethyl complex, the SBLCT transitions are still lowered in energy, due to the weakening of the metal–R bond, but the excitation energies to the MLCT states are not significantly affected. This is a consequence of the more covalent character of the metal–ethyl bond as compared to the metal–methyl bond. The substitution of hydrogen by an alkyl group is accompanied not only by a red shift of the low-lying MLCT states from 15 090–26 000 to 13 690–20 410 cm^{-1} but also by an increase in the density of states in the visible energy domain. The second effect that will affect the photophysics and the photochemistry within the molecular series implies an important mixing between the MLCT and SBLCT excited states. A comparison between the lowest part of the spectrum of $Mn(H)(CO)_3(H-DAB)$ and $Re(H)(CO)_3(H-DAB)$ points to a large influence of the metal center, mainly due to the relativistic destabilization of the d shells and the stabilizing interaction between the π^*_{DAB} and the $6p_z$ of the metal center. The consequences are a stabilization of the excited states calculated between 12 600–27 650 cm^{-1} (triplet components) and 15 250–31 340 cm^{-1} (singlet components) and a significant mixing between the MLCT and SBLCT states.

1. Introduction

Quite recently, the spectroscopy, photophysics, and photochemistry of a series of complexes $M(L)(CO)_3(\alpha\text{-diimine})$ ($M = Mn, Re$), in which L represents a metal fragment or an alkyl group bound to the metal by a high-lying σ orbital, have been studied in detail.^{1–8} From these studies, it was concluded that

mainly $d_\pi(M) \rightarrow \pi^*(\alpha\text{-diimine})$ (metal-to-ligand-charge-transfer: MLCT) transitions contribute to the absorption spectra, but that decay to the ground state and homolytic cleavage of the metal–L bond take place from a close low-lying $\sigma_{M-L} \rightarrow \pi^*$ ($\alpha\text{-diimine}$) (sigma-bond-to-ligand-charge-transfer: ${}^3\sigma\pi^*$ or ${}^3\text{-SBLCT}$) excited state. To rationalize the experimental data, a few theoretical investigations, based either on DFT calculations^{9,10} or on accurate CASSCF/MR-CCI calculations,^{11,12} have

[†] Laboratoire de Chimie Quantique.

[‡] Anorganisch Chemisch Laboratorium.

- (1) Stufkens, D. J. *Comments Inorg. Chem.* **1992**, *13*, 359.
- (2) Rossenaar, B. D.; van der Graaf, T.; van Eldik, R.; Langford, C. H.; Stufkens, D. J.; Vlček, A., Jr. *Inorg. Chem.* **1994**, *33*, 2865.
- (3) Rossenaar, B. D.; Kleverlaan, C. J.; Stufkens, D. J.; Oskam, A. J. *Chem. Soc., Chem. Commun.* **1994**, 63.
- (4) van Outersterp, J. W. M.; Stufkens, D. J.; Vlček, A., Jr. *Inorg. Chem.* **1995**, *34*, 5183.
- (5) Rossenaar, B.; Lindsay, E.; Stufkens, D. J.; Vlček, A., Jr. *Inorg. Chim. Acta* **1996**, *250*, 5.

- (6) Rossenaar, B. D.; George, M. W.; Johnson, F. P. A.; Stufkens, D. J.; Turner, J. J.; Vlček, A., Jr. *J. Am. Chem. Soc.* **1995**, *117*, 11582.
- (7) Rossenaar, B. D.; Kleverlaan, C. J.; van de Ven, M. C. E.; Stufkens, D. J.; Vlček, A., Jr. *Chem. Eur. J.* **1996**, *2*, 228.
- (8) Rossenaar, B. D.; Stufkens, D. J.; Oskam, A.; Fraanje, J.; Goubitz, K. *Inorg. Chim. Acta* **1996**, *247*, 215.
- (9) Aarnts, M. P.; Stufkens, D. J.; Wilms, M. P.; Baerends, E. J.; Vlček, A., Jr.; Clark, I. P.; George, M. W.; Turner, J. J. *Chem. Eur. J.* **1996**, *2*, 1556.

been performed. Recently, the potential energy curves corresponding to the ¹A' electronic ground state and to the low-lying ³A' excited states have been computed for the model complex Mn(H)(CO)₃(H-DAB) as a function of $q_a = [\text{Mn}-\text{H}]$ and $q_b = [\text{Mn}-\text{CO}_{\text{ax}}]$ under the C_s symmetry constraint.¹³ The interaction between the quasi-bound MLCT excited states and the SBLCT excited state, which is dissociative with respect to the metal-hydrogen bond, is the key to the photochemical behavior of this class of molecules. The presence of energy barriers due to avoided crossings between the two ³MLCT states and the ³-SBLCT state at the early stage of the Mn-H homolysis prevents the occurrence of this reaction in the hydride complex.

For the $\sigma(\text{M}-\text{L})$ -bonded M(L)(CO)₃(α -diimine) complexes in general, the quantum yield and the time scale of the homolysis will depend on the factors (wavelength of irradiation, nature of the radical species to be produced, metal center and π acceptor ligand) governing the facility with which the system overcomes these energy barriers. Depending on heights of the barriers (or on the relative position of the ³SBLCT and ³MLCT excited states), two different opposite channels are open: (i) an ultrafast direct dissociation (less than 100 fs) with 100% of the system dissociating into the radicals and (ii) a nonradiative transition to the vibrationally excited levels of the ³MLCT states followed by decay to the ground state. An illustration of this unconventional photochemical/photophysical behavior has been recently reported for a number of complexes. For instance, whereas the homolysis of M(R)(CO)₃(R'-DAB) (M = Re, R = ethyl, benzyl; M = Mn, R = benzyl; R' = isopropyl, *p*-tolyl) is characterized by a quantum yield close to 1, the methyl analogues do not show significant homolysis upon visible excitation ($\phi \approx 10^{-2}$ for M = Re,⁷ $\phi = 0$ for M = Mn⁸). When the R'-DAB ligand is replaced by a 4,4-Me₂-bipyridine (bpy') to give Re(R)(CO)₃(bpy'), the branching ratios between the homolysis and the unproductive decay to the electronic ground state are 0.40/0.60 and 1.0/0.0 for the methyl and the ethyl complexes, respectively.¹⁴

The aim of the present study is to determine the relative order of the transitions to the low-lying singlet and triplet A' excited states (MLCT, SBLCT, MC) of the molecules Mn(R)(CO)₃(H-DAB) with R = hydrogen, methyl, and ethyl and of Re(H)(CO)₃(H-DAB), through contracted configuration interaction (CCI) calculations based on complete active space SCF (CASSCF) reference wave functions. The rationalization of the influence of the R group and of the metal center on the photophysical/photochemical properties of the M(R)(CO)₃(α -diimine) complexes is the ultimate goal of this kind of study.

2. Computational Method

The model complexes have the conformation depicted in Figure 1. The calculations were performed under the C_s symmetry constraint for the ¹A' electronic ground state corresponding to the

$$(\sigma_{\text{Mn}-\text{R}})^2(\text{nd}_{x^2-y^2})^2(\text{nd}_{yz})^2(\text{nd}_{xz})^2$$

electronic configuration ($n = 3$ for the manganese complex, $n = 5$ for the rhenium) and for the low-lying ^{1,3}A' excited states corresponding

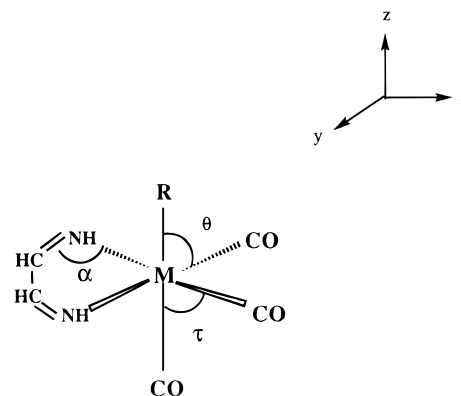


Figure 1. Idealized geometry of M(R)(CO)₃(H-DAB) (M = Mn, R = H, CH₃, C₂H₅; M = Re, R = H).

to the $3d_{xz} \rightarrow \pi^*_{\text{DAB}}$, $3d_{x^2-y^2} \rightarrow \pi^*_{\text{DAB}}$, $\sigma_{\text{Mn}-\text{R}} \rightarrow \pi^*_{\text{DAB}}$, and $3d_{yz} \rightarrow 3d_{xy}$ excitations in Mn(R)(CO)₃(H-DAB) and to the low-lying ¹A' excited states corresponding to the $5d_{xz} \rightarrow \pi^*_{\text{DAB}}$, $5d_{x^2-y^2} \rightarrow \pi^*_{\text{DAB}}$, and $\sigma^*_{\text{Re}-\text{H}} \rightarrow \pi^*_{\text{DAB}}$ excitations in Re(H)(CO)₃(H-DAB). Idealized geometries were deduced from the ground-state structures of MnCl(CO)₃(Ph-DAB) (Ph = phenyl)¹⁵ of Mn(H)(CO)₅¹⁶ and from Re(Me)(CO)₃(ⁱPr-DAB)¹⁷ with the following bond lengths and bond angles.

For Mn(H)(CO)₃(H-DAB): Mn-H = 1.576 Å; Mn-CO_{ax} = 1.820 Å; Mn-CO_{eq} = 1.807 Å; H-DAB: Mn-N = 2.032 Å; N-C = 1.280 Å; C-C = 1.508 Å; N-H = 1.010 Å; C-H = 1.080 Å.

For Mn(R)(CO)₃(H-DAB) with R = CH₃ and C₂H₅: Mn-C_{alkyl} = 2.190 Å; C-C_{ethyl} = 1.520 Å, the angles τ , θ , and α being kept constant at 90°, 96°, and 117, 5°, respectively. For Re(H)(CO)₃(H-DAB): Re-H = 1.799 Å; Re-CO = 2.000 Å. H-DAB: Re-N = 2.177 Å, the angles τ , θ , and α being kept constant at 96.3°, 98°, and 113, 1°, respectively.

In a recent work,¹⁸ we have shown that the geometrical structure of Mn(H)(CO)₃(H-DAB) is not dramatically affected on going from the electronic ground state to the lowest triplet excited states. The main structural deformations observed, at the CASSCF level using a gradient method, are an elongation of the Mn-CO_{ax} bond in the lowest ³MLCT excited state (1.918 Å in the ground state vs 2.235 Å in the excited state) and an elongation of the Mn-H bond in the ³SBLCT excited state (1.625 Å in the ground state vs 1.946 Å in the excited state), the main angular deformations being less than 10° and the other interatomic distances being only slightly affected. We have shown that these bond elongations are directly connected to the dissociative character of the MLCT and SBLCT states for the axial CO loss and the Mn-H bond homolysis, respectively.¹³

On the basis of these results, a systematic geometry optimization of the triplet excited states is not justified. Moreover, in the present work, we are primarily interested in vertical transitions in the Franck-Condon domain where the system has no time to relax to form stationary states. In principle, triplet states can be populated upon transitions either directly from the ground state (in the presence of heavy atoms) or by intersystem crossing from upper singlet states.¹⁹ The time scale for these events are very small (fs to ps) as compared with the relaxation to the vibrational ground states of the triplets (ps to ns time scale). A recent time-resolved spectroscopy study of [Ru(bpy)₃]²⁺ has shown that the absorption spectrum is resolved in less than 200 fs.²⁰ Clearly, the investigation of other photophysical properties connected to long-lived

- (10) Aarnts, M. P.; Wilms, M. P.; Peelen, K.; Fraanje, J.; Goubitz, K.; Hartl, F.; Stufkens, D. J.; Baerends, E. J.; Vlcek, A., Jr. *Inorg. Chem.* **1996**, *35*, 5468.
- (11) Daniel, C.; Matsubara, T.; Stor, G. *Coord. Chem. Rev.* **1994**, *132*, 63.
- (12) Finger, K.; Daniel, C. *J. Chem. Soc. Chem. Commun.* **1995**, 63.
- (13) Finger, K.; Daniel, C. *Coord. Chem. Rev.*, in press.
- (14) Finger, K.; Daniel, C. *J. Am. Chem. Soc.* **1995**, *117*, 12322.
- (15) Kleverlaan, C. J.; Stufkens, D. J.; Clark, I. P.; George, M. W.; Turner, J. J.; Martino, D. M.; van Willigen, H.; Vlcek, A., Jr. Submitted to *J. Am. Chem. Soc.*

- (15) Schmidt, G. S.; Paulus, H.; van Eldik, R.; Elias, H. *Inorg. Chem.* **1988**, *27*, 3211.
- (16) McNeill, E. A.; Schöler, F. R. *J. Am. Chem. Soc.* **1977**, *99*, 6243.
- (17) Rossenaar, B. D.; Kleverlaan, C. J.; van de Ven, M. C. E.; Stufkens, D. J.; Oskam, A.; Fraanje, J.; Goubitz, K. *J. Organomet. Chem.* **1995**, *493*, 153.
- (18) Guillaumont, D.; Daniel, C. *Chem. Phys. Lett.* **1996**, *257*, 1.
- (19) Daniel, C.; Heitz, M. C.; Manz, J.; Ribbing, C. *J. Chem. Phys.* **1995**, *102* (2), 905. Heitz, M. C.; Ribbing, C.; Daniel, C. *J. Chem. Phys.* **1997**, *106* (4), 1421.
- (20) McCusker, J. K. 12th ISPPCC, Colchester, VT, 1997.

Table 1. CASSCF/MR-CCI Excitation Energies (in cm^{-1}) to the Low-Lying ${}^1A'$ Excited States of $\text{Mn}(\text{R})(\text{CO})_3(\text{DAB})$ (R = H, methyl, ethyl) and Corresponding Oscillator Strengths; the CI Coefficients Are Given in Parentheses

transition	R = H		R = CH ₃		R = C ₂ H ₅	
$a^1A' \rightarrow a^3A'$	MLCT	15 090	MLCT/SBLCT	12 415	MLCT/SBLCT	13 690
	$3d_{xz} \rightarrow \pi^*_{\text{DAB}}$ (0.90)	16 050 ^a	$3d_{xz}/\sigma_{\text{Mn-R}} \rightarrow \pi^*_{\text{DAB}}$ (0.88)	12 730 ^c	$3d_{xz}/\sigma_{\text{Mn-R}} \rightarrow \pi^*_{\text{DAB}}$ (0.87)	11 080 ^c
		16 140 ^b	$\sigma_{\text{Mn-R}}/3d_{xz} \rightarrow \pi^*_{\text{DAB}}$ (0.16)		$\sigma_{\text{Mn-R}}/3d_{xz} \rightarrow \pi^*_{\text{DAB}}$ (0.24)	
$a^1A' \rightarrow b^3A'$	MLCT	19 200	MLCT	15 540	MLCT	16 860
	$3d_{x^2-y^2} \rightarrow \pi^*_{\text{DAB}}$ (0.88)	19 900 ^a	$3d_{x^2-y^2} \rightarrow \pi^*_{\text{DAB}}$ (0.82)	16 820 ^c	$3d_{x^2-y^2} \rightarrow \pi^*_{\text{DAB}}$ (0.85)	16 200 ^c
$a^1A' \rightarrow b^1A'$	MLCT ($f = 0.03$)	21 060	MLCT ($f = 0.01$)	17 090	MLCT	17 090
	$3d_{x^2-y^2} \rightarrow \pi^*_{\text{DAB}}$ (0.90)	21 710 ^a	$3d_{x^2-y^2} \rightarrow \pi^*_{\text{DAB}}$ (0.85)	20 430 ^c	$3d_{x^2-y^2} \rightarrow \pi^*_{\text{DAB}}$ (0.88)	17 560 ^c
		18 300 ^b				
$a^1A' \rightarrow c^1A'$	MLCT ($f = 0.39$)	26 000	MLCT/SBLCT ($f = 0.24$)	22 540	MLCT/SBLCT	20 410
	$3d_{xz} \rightarrow \pi^*_{\text{DAB}}$ (0.75)	26 630 ^a	$\sigma_{\text{Mn-R}}/3d_{xz} \rightarrow \pi^*_{\text{DAB}}$ (0.65)	23 050 ^c	$3d_{xz}/\sigma_{\text{Mn-R}} \rightarrow \pi^*_{\text{DAB}}$ (0.76)	15 580 ^c
		23 000 ^b	$3d_{xz}/\sigma_{\text{Mn-R}} \rightarrow \pi^*_{\text{DAB}}$ (0.48)		$\sigma_{\text{Mn-R}}/3d_{xz} \rightarrow \pi^*_{\text{DAB}}$ (0.38)	
$a^1A' \rightarrow c^3A'$	MC	26 380	MC	21 470	MC	22 900
	$3d_{yz} \rightarrow 3d_{xy}$ (0.76)		$3d_{yz} \rightarrow 3d_{xy}$ (0.78)		$3d_{yz} \rightarrow 3d_{xy}$ (0.78)	
$a^1A' \rightarrow d^3A'$	SBLCT	34 390	SBLCT/MLCT	21 790	SBLCT/MLCT	19 670
	$\sigma_{\text{Mn-H}} \rightarrow \pi^*_{\text{DAB}}$ (0.89)		$\sigma_{\text{Mn-R}}/3d_{xz} \rightarrow \pi^*_{\text{DAB}}$ (0.84)	22 900 ^c	$\sigma_{\text{Mn-R}}/3d_{xz} \rightarrow \pi^*_{\text{DAB}}$ (0.82)	
			$3d_{xz}/\sigma_{\text{Mn-R}} \rightarrow \pi^*_{\text{DAB}}$ (-0.25)		$3d_{xz}/\sigma_{\text{Mn-R}} \rightarrow \pi^*_{\text{DAB}}$ (-0.25)	
$a^1A' \rightarrow d^1A'$	MC ($f = 0.02$)	35 900	SBLCT/MLCT ($f = 0.21$)	31 050	SBLCT/MLCT	25 620
	$3d_{yz} \rightarrow 3d_{xy}$ (0.66)		$3d_{xz}/\sigma_{\text{Mn-R}} \rightarrow \pi^*_{\text{DAB}}$ (-0.65)	28 200 ^c	$\sigma_{\text{Mn-R}}/3d_{xz} \rightarrow \pi^*_{\text{DAB}}$ (0.71)	26 240 ^c
			$\sigma_{\text{Mn-R}}/3d_{xz} \rightarrow \pi^*_{\text{DAB}}$ (0.51)		$3d_{xz}/\sigma_{\text{Mn-R}} \rightarrow \pi^*_{\text{DAB}}$ (0.48)	
$a^1A' \rightarrow e^1A'$	SBLCT ($f = 0.11$)	37 950	MC ($f = 0.01$)	32 440	MC	34 200
	$\sigma_{\text{Mn-H}} \rightarrow \pi^*_{\text{DAB}}$ (0.80)		$3d_{yz} \rightarrow 3d_{xy}$ (0.82)		$3d_{yz} \rightarrow 3d_{xy}$ (0.78)	

^a From ref 13. ^b Calculations including more reference configurations in the CCI. ^c Calculations with limited basis set II.

excited states (e.g., emission spectra) should take into account the relaxation effects neglected in this study.

The following Gaussian basis sets were used for $\text{Mn}(\text{R})(\text{CO})_3(\text{H-DAB})$ in an all-electron calculation scheme: for the manganese atom a (15,11,6) set contracted to [9,6,3],²¹ for the first-row atoms a (10,6) set contracted to [4,2],²⁴ for the hydrogen atom either a (6,1) set contracted to [3,1]²⁵ (for the atom directly linked to the metal center) or a (4) set contracted to [2]²⁴ for the other hydrogen atoms. For the rhenium complex, studied in the relativistic effective core potential (ECP) (small core) approximation, the following Gaussian basis sets were used: for the rhenium atom ($Z = 15.0$) a (8,7,6) set contracted to [6,5,3],²⁶ for the carbon ($Z = 4.0$) and nitrogen ($Z = 5.0$) atoms a (4,4) set contracted to [2,2],²⁷ and for oxygen ($Z = 6.0$) atoms a (4,5) set contracted to [2,3].²⁷ The same basis sets were used for the hydrogen atoms in the manganese and rhenium complexes.

The choice of the method has been motivated by our experience in excited-state calculations of coordination compounds with low symmetry and a number of low-lying interacting electronic states for which single-determinantal (DFT) or perturbative (CASPT2) approaches are inadequate. CASSCF calculations²⁸ were carried out to obtain wave functions which are used as references in the multireference CCI calculations.²⁹ CASSCF calculations averaged over five low-lying states of a given symmetry and spin were performed in order to generate a set of molecular orbitals used in a subsequent multireference CI. Since our interest centers mostly on the lowest excited states corresponding

to $nd \rightarrow \pi^*_{\text{DAB}}$, $nd \rightarrow nd$, and $\sigma_{\text{Mn-R}} \rightarrow \pi^*_{\text{DAB}}$ excitations, eight electrons are correlated (the nd electrons and the two electrons involved in the Mn-R bond) in 10 orbitals corresponding to the nd and nd' orbitals which correlate them, the $\sigma_{\text{Mn-R}}$ and $\sigma^*_{\text{Mn-R}}$ orbitals ($\sigma_{\text{Mn-R}}$ and $\sigma^*_{\text{Mn-R}}$ denote the molecular orbitals that are bonding and antibonding with respect to the Mn-R bond, respectively), and the lowest π^*_{DAB} localized on the DAB group. For each electronic state a monoreference CCI calculation is performed followed by a multireference, including all configurations that appear with a coefficient larger than 0.08 in the monoreference CI (the number of references may vary from 4 to 12 states). Single and double excitations to all virtual orbitals, except the counterparts of the carbonyls and diimine 1s and of the metal 1s, 2s, and 2p orbitals, are included. The number of configurations ranged from 250 000 to 1 000 000, but this number is reduced to at most a few thousands by contraction. The integral calculations were carried out either with the system of programs ARGOS³¹ or with the system of programs ASTERIX.³⁰ Some of the calculations were performed with the system of programs MOLCAS 3.0.³²

3. Results and Discussion

Mn(H)(CO)₃(H-DAB) Excited States. The calculated excitation energies to the lowest ${}^1A'$ of $\text{Mn}(\text{H})(\text{CO})_3(\text{H-DAB})$ are collected in Table 1. The relative position of the different types of singlet excited states (MC, SBLCT, MLCT) is represented in Figure 2 (left side).

The transitions to the lowest singlet excited states are calculated at 21 060 and 26 000 cm^{-1} . These two, nearly pure, MLCT transitions, corresponding to the $3d_{x^2-y^2} \rightarrow \pi^*_{\text{DAB}}$ and $3d_{xz} \rightarrow \pi^*_{\text{DAB}}$ excitations, are well separated ($\Delta E = 5000 \text{ cm}^{-1}$). Very different oscillator strengths, 0.03 and 0.39, respectively, characterize these low-lying singlets. A strong interaction between the electronic ground state and the c^1A' ($3d_{xz} \rightarrow \pi^*_{\text{DAB}}$) state raises the latter one into the high-energy domain ($> 20\,000 \text{ cm}^{-1}$). This is illustrated by the large energy gap between the

(21) This basis set is made from the (14, 9, 5) basis set of Wachters,²² by adding an additional s function (exponent 0.3218), two diffuse p functions, and one diffuse d function. All the exponents were chosen according to the even-tempered criterion of Raffanetti.²³

(22) Wachters, A. J. H. *J. Chem. Phys.* **1970**, *52*, 1033.

(23) Raffanetti, R. C.; Bardo, R. D.; Ruedenberg, K. In *Energy Structure and Reactivity*; Smith, D. W., Mc Rae, W. B., Eds.; Wiley: New York, 1973; p 164.

(24) Huzinaga, S. *Approximate Atomic Functions*: technical report; University of Alberta, Canada, 1971.

(25) Huzinaga, S. *J. Chem. Phys.* **1965**, *42*, 1293.

(26) Andrae, D.; Haussermann, U.; Dolg, M.; Stoll, H.; Preuss, H. *Theor. Chim. Acta* **1990**, *77*, 123.

(27) Bergner, A.; Dolg, M.; Kuechle, W.; Stoll, H.; Preuss, H. *Mol. Phys.* **1993**, *80*, 1431.

(28) Siegbahn, P. E. M.; Almlöf, J.; Heiberg, A.; Roos, B. O. *J. Chem. Phys.* **1981**, *74*, 2384.

(29) Siegbahn, P. E. M. *Int. J. Quantum Chem.* **1983**, *23*, 1869. The original program was interfaced for use in conjunction with the ASTERIX system of programs³⁰ by Daniel, C.; Spéri, M.; Rohmer, M. M.

(30) Ernenwein, R.; Rohmer, M. M.; Bénard, M. *Comput. Phys. Commun.* **1990**, *58*, 305; Wiest, R.; Demuyneck, J.; Bénard, M.; Rohmer, M. M.; Ernenwein, R. *Comput. Phys. Commun.* **1991**, *62*, 107.

(31) Pitzer, R. J. *J. Chem. Phys.* **1973**, *58*, 3111.

(32) Andersson, K.; Blomberg, M. R. A.; Fülcher, M. P.; Karström, G.; Kellö, V.; Lindh, R.; Malmqvist, P.-Å.; Noga, J.; Olsen, J.; Roos, B. O.; Sadlej, A. J.; Siegbahn, P. E. M.; Urban, M.; Widmark, P.-O. *MOLCAS-3.0*; University of Lund: Sweden.

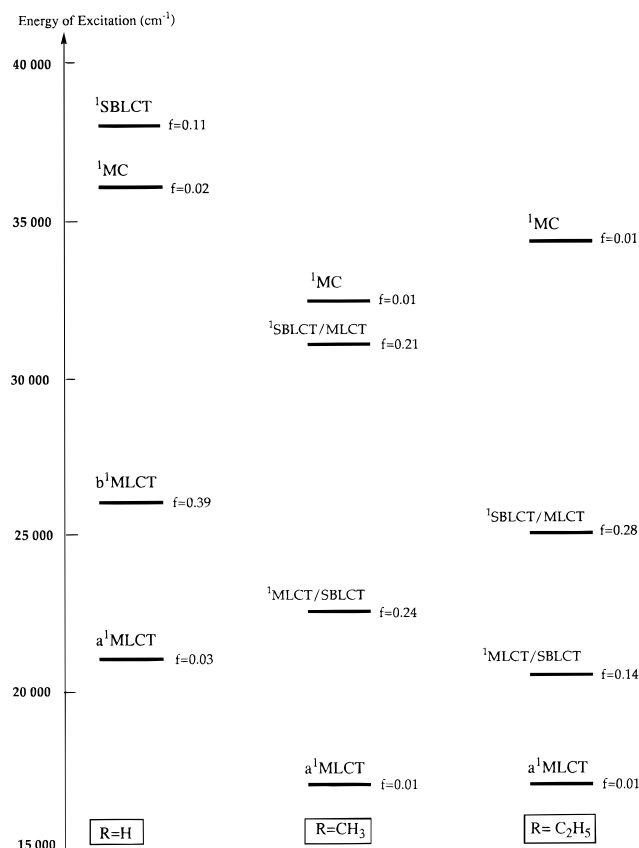


Figure 2. Relative position of the low-lying $^1A'$ excited states of $Mn(R)(CO)_3(H-DAB)$ as a function of $R = H, CH_3, C_2H_5$ (f represents the oscillator strength).

singlet and triplet MLCT ($3d_{xz} \rightarrow \pi^*_{DAB}$) transitions of ca. $11\,000\text{ cm}^{-1}$ and by a reverse order of the singlet states with respect to the corresponding triplet states. This large $a^3A' - c^1A'$ energy gap is much larger than the singlet–triplet energy difference calculated for the other MLCT transition ($3d_{x^2-y^2} \rightarrow \pi^*_{DAB}$) (2200 cm^{-1}). The oscillator strengths, calculated at the CASSCF level and reported in Table 1, indicate that the excitation to the higher 1MLCT state ($3d_{xz} \rightarrow \pi^*_{DAB}$) is more likely populated under irradiation in the visible. The metal-centered transition corresponding to $3d_{yz} \rightarrow 3d_{xy}$ excitation is calculated at $26\,380\text{ cm}^{-1}$ (triplet) and $35\,900\text{ cm}^{-1}$ (singlet) with an oscillator strength of 0.02, thus giving rise to an expected very weak absorption. The highest singlet excited state, calculated at $37\,950\text{ cm}^{-1}$, corresponds mainly to the $\sigma_{Mn-R} \rightarrow \pi^*_{DAB}$ excitation with a nonnegligible contribution of the electronic ground state (6%). An intermediate oscillator strength ($f = 0.11$) makes it a good candidate for population by near-UV irradiation. The corresponding SBLCT triplet state is calculated at $34\,390\text{ cm}^{-1}$ and is nearly pure.

We will now compare the calculated excitation energies of the hydride complex with the previous results (see Table 1) obtained for this molecule with a different computational strategy.¹³ In the previous work, the CASSCF wave functions were optimized independently for each electronic state, and the subsequent CI treatment was performed in the same way as in the present study. The largest deviation is observed for the singlet and triplet metal-centered states for which the CI coefficients are smaller than 0.80, indicating a significant mixing with other electronic states. Consequently, an important correction to the excitation energies is expected when taking into account these interactions at an average CASSCF level.³³ The other excited states are only slightly affected by the

change of reference wave function (a unique CASSCF for each state or an average CASSCF over several states of a given symmetry).

Finally, some of the excited states reported in Table 1 for the hydride have been recalculated with an enlarged reference space in the MR/CCI calculations. This approach was used for the computation of the two-dimensional potential energy surfaces (PES) for the hydrogen and the axial carbonyl ligand dissociations.³⁴ Whereas the triplet states, for which only a few reference configurations are added in this more refined treatment, are not significantly affected, one observes an appreciable lowering of the transitions to the two lowest 1MLCT states by 3000 cm^{-1} . As a result, these transitions, corresponding to $3d_{x^2-y^2} \rightarrow \pi^*_{DAB}$ and $3d_{xz} \rightarrow \pi^*_{DAB}$ excitations, are calculated at $18\,300$ and $23\,000\text{ cm}^{-1}$, respectively. These values are in excellent agreement with the main features of the absorption spectra reported for this class of molecules. For instance, the complex $Mn(Me)(CO)_3(Pr-DAB)$ has an intense absorption band in benzene at $19\,500\text{ cm}^{-1}$.⁸

$Mn(R)(CO)_3(H-DAB)$ ($R = CH_3, C_2H_5$) Excited States. The calculated CASSCF/MR-CCI excitation energies to the lowest $^1,^3A'$ of the methyl and ethyl manganese compounds are reported in Table 1. For both molecules, two calculations have been performed: one with basis set I described in the computational strategy section, the other with a smaller basis set, called basis set II (for the manganese atom a (14,9,6) set contracted to [6,4,3],³⁵ for the second-row atoms a (9,5) set contracted to [3,2]²⁴). The excitation energies obtained with basis set I are directly comparable to the values reported for the hydride complex. Whereas the change of basis sets does not affect dramatically the excitation energies and the relative order of the excited states in $Mn(R)(CO)_3(H-DAB)$, it may substantially influence their descriptions. Whereas the transitions obtained with basis set I are described by a significant mixing between the so-called MLCT and SBLCT states corresponding to $3d_{xz} \rightarrow \pi^*_{DAB}$ and $\sigma_{Mn-R} \rightarrow \pi^*_{DAB}$ excitations, respectively (see discussion below), the calculations performed with basis set II do not show any important mixing for the singlet states.³⁷ The important role of the $4p_z$ orbital of the metal center in the $3d_{xz}/3d_{z^2}$ hybridization that accompanies this mixing could explain this basis set effect.

The relative position of the low-lying singlet excited states of $Mn(R)(CO)_3(H-DAB)$ as a function of $R = H, CH_3, C_2H_5$ is represented in Figure 2.

On going from the hydride to the methyl complex the main trends are (i) a lowering of the different excited states (MLCT, SBLCT, and MC) and (ii) a strong mixing between the so-called MLCT and SBLCT excited states. Replacing the methyl ligand by an ethyl group gives rise to (i) a decrease in energy of the SBLCT transitions, an increase in energy of the MC ones, and small changes in the energies of the MLCT transitions and (ii) the conservation of the mixed MLCT/SBLCT character.

The three-center character (Scheme 1) of the radical/metal/DAB interaction is responsible for these large effects on the

(33) Hachey, M. R. J.; Daniel, C. *Inorg. Chem.* **1998**, *37* (6), 1387.

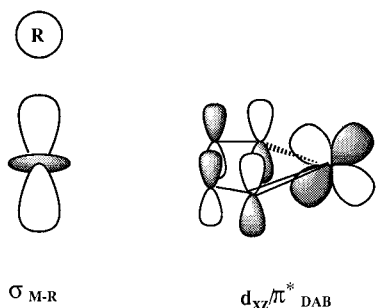
(34) Guillaumont, D. Ph.D. Thesis, Strasbourg, France, 1998.

(35) This basis set is made from the (13, 7, 5) set of ref 36 by adding one s function (exponent 0.2732) and two p functions (exponents 0.2021 and 0.065 16) and replacing the last d function with two d functions (exponents 0.2584 and 0.082 31).

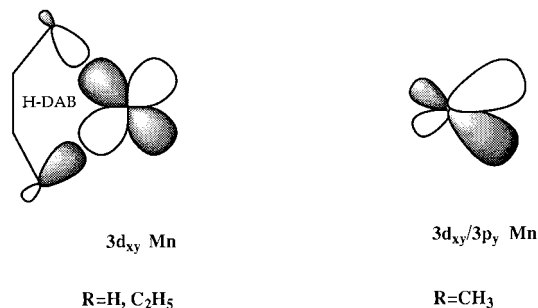
(36) Hyla-Kryspin, I.; Demuyck, J.; Strich, A.; Bénard, M. *J. Chem. Phys.* **1981**, *75*, 3954.

(37) Guillaumont, D.; Finger, K.; Hachey, M. R. J.; Daniel, C. *Coord. Chem. Rev.* **1998**, *171*, 439.

Scheme 1



Scheme 2



excitation energies and on the nature of the excited states. In fact, the evolution of this interaction within this series of molecules is governed by three main features: (i) the strength of the $\sigma_{\text{Mn-R}}$ bond ($\text{Mn-H} > \text{Mn-CH}_3 > \text{Mn-C}_2\text{H}_5$); (ii) the basicity of the R group ($\text{C}_2\text{H}_5^- \geq \text{CH}_3^- > \text{H}^-$); (iii) the more or less polarized character of this bond ($\text{Mn-CH}_3 > \text{Mn-H} > \text{Mn-C}_2\text{H}_5$). The π^*_{DAB} acceptor ligand will adapt its behavior (more or less acceptor) to the nature of the R group on the basis of the electronic density available on the metal center. To analyze the main features reported in Table 1, we must take into account the following qualitative trends within the molecular series.

The consequence of the weakening of the M-R bond, when the hydrogen is replaced by a methyl or ethyl group, is a destabilization of the $\sigma_{\text{M-R}}$ bonding orbital and a stabilization of the π^*_{DAB} orbitals due to a stronger metal-DAB stabilizing interaction. Consequently, both the SBLCT and the MLCT states should be stabilized.

On going from the hydride to the methyl complex, both the basicity and the polarized character of the Mn-R bond increase. The main consequence is a decrease of the electronic density on the metal center, which should be accompanied by a stabilization of the 3d orbitals. However, this expected stabilization of the 3d occupied orbitals is offset by very weak $3d/\pi^*_{\text{DAB}}$ and $3d/\pi^*_{\text{COeq}}$ stabilizing interactions due to the lack of density on the metal center. In contrast, the vacant $3d_{xy}$ orbital is largely stabilized by its hybridization with the $4p_y$ orbital, preventing the σ antibonding interaction with the H-DAB group (Scheme 2). The net result will be a lowering of both MLCT and MC excited states.

When the methyl is replaced by an ethyl group, the main change, apart from the weakening of the Mn-R bond, is a decrease of the polarization of the bond, by which it becomes more "covalent". The principal consequence will be an increase of the electronic density of the metal center, causing a destabilization of the $3d_{xy}$ vacant orbital (Scheme 2) and a stabilization of the 3d occupied orbitals by interaction with the π^*_{DAB} and π^*_{COeq} . Consequently, the transition energies to the MLCT and MC states should increase.

The weakening of the metal-R bond is illustrated by an important lowering of the SBLCT states on going from the hydride ($34\,390\text{ cm}^{-1}$ (triplet) and $37\,950\text{ cm}^{-1}$ (singlet)) to the methyl ($21\,790\text{ cm}^{-1}$ (triplet) and $31\,050\text{ cm}^{-1}$ (singlet)) and to the ethyl ($19\,000\text{ cm}^{-1}$ (triplet) and $25\,620\text{ cm}^{-1}$ (singlet)). The two low-lying singlet states are red shifted by at least 0.5 eV when the hydrogen is replaced by a methyl radical. Whereas the lowest singlet excited state, corresponding to the $3d_{x^2-y^2} \rightarrow \pi^*_{\text{DAB}}$ excitation, is purely MLCT in character in the three molecules, the next one has a mixed MLCT/SBLCT character in the methyl ($22\,540\text{ cm}^{-1}$) and ethyl ($20\,410\text{ cm}^{-1}$) complexes. The same trend is observed for the corresponding triplet states but with a less important mixing (see the CI coefficients in Table 1). This mixing, occurring both at the molecular orbital level and at the state configuration level, makes a definitive assignment difficult. The SBLCT/MLCT counterpart of this excited state is calculated at $31\,050\text{ cm}^{-1}$ ($\text{R} = \text{CH}_3$) and $25\,620\text{ cm}^{-1}$ ($\text{R} = \text{C}_2\text{H}_5$).

The MC excited states remain nearly pure in the molecular series, but their energies are drastically lowered on going to the methyl complex. They are calculated at $21\,470\text{ cm}^{-1}$ (vs $26\,380\text{ cm}^{-1}$ in the hydride complex) and $32\,440\text{ cm}^{-1}$ (vs $35\,900\text{ cm}^{-1}$ in the hydride complex) for the triplet and singlet components, respectively. This substantial energy stabilization is attributed to the more polarized character of the Mn-CH₃ bond as compared with that of the Mn-H bond. Due to the more "ionic" character of the Mn-R bond in $\text{Mn}(\text{CH}_3)(\text{CO})_3$ (H-DAB), the vacant $3d_{xy}$ orbital is stabilized by its hybridization with the $4p_y$ of the metal, leading to a better overlap with the equatorial carbonyls and to a reduction of the σ antibonding overlap with the DAB ligand (Scheme 2). In contrast, one observes an increase in the excitation energies of the MC states on going from the methyl to the ethyl due to the more covalent nature of the Mn-ethyl bond.

In the ethyl complex two effects, weakening of the metal-R bond and polarization of the bond, act in opposite direction as far as the MLCT transitions are concerned. Whereas a weakening of the Mn-R bond causes a stabilization of these states, these states will be in turn destabilized by the less polarized character of this bond. Consequently, the excitation energies to the MLCT states are not dramatically modified on going from the methyl to the ethyl complex, as can be seen from Table 1. This is illustrated by the similar excitation energies obtained for the three low-lying excited states either with a pure MLCT ($3d_{x^2-y^2} \rightarrow \pi^*_{\text{DAB}}$) or with a pronounced MLCT character (a^3A') on going from the methyl to the ethyl complex. The b^1A' excited state adopts an intermediate behavior (lowering of 2000 cm^{-1}) since it is characterized by a large contribution of the SBLCT state.

The oscillator strengths of the transitions to the lowest $^1\text{MLCT}$ ($f = 0.03/0.01$) and the ^1MC ($f = 0.02/0.01$) states are very similar for the hydride and the alkyl complexes. The mixing between two states of different natures, MLCT and SBLCT, is illustrated by the intermediate oscillator strengths of the methyl complex ($f = 0.24$ for the MLCT/SBLCT transition calculated at $22\,540\text{ cm}^{-1}$, and $f = 0.21$ for the SBLCT/MLCT transition calculated at $31\,050\text{ cm}^{-1}$). For comparison, values of 0.39 and 0.11 are obtained for the transitions to the pure MLCT and SBLCT states of the hydride complex, respectively. The mixed MLCT/SBLCT character of the low-lying states in the substituted alkyl complexes, either contributing to the absorption spectrum (singlet components) or involved in the photodissociation dynamics, could lead to substantial distortions of the shape of the associated potentials with large consequences on

Table 2. Calculated CASSCF/CCI Excitation Energies (in cm⁻¹) to the Lowest ^{1,3}A' Excited States of HRe(CO)₃(DAB)

transition	one-electron excitation in the principal configurations	
a ¹ A' → a ³ A'	5d _{xz} + σ _{Re-H} → π _{DAB} * (0.71) σ _{Re-H} - 5d _{xz} → π _{DAB} * (0.64) MLCT/SBLCT	12 600
a ¹ A' → b ³ A'	5d _{x²-y²} → π _{DAB} * (0.90) MLCT	13 710
a ¹ A' → b ¹ A'	5d _{x²-y²} → π _{DAB} * (0.91) MLCT (f = 0.0003)	15 250
a ¹ A' → c ¹ A'	5d _{xz} + σ _{Re-H} → π _{DAB} * (0.68) σ _{Re-H} - 5d _{xz} → π _{DAB} * (0.44) MLCT/SBLCT (f = 0.32)	21 720
a ¹ A' → c ³ A'	σ _{Re-H} - 5d _{xz} → π _{DAB} * (0.69) 5d _{xz} + σ _{Re-H} → π _{DAB} * (0.59) SBLCT/MLCT	27 650
a ¹ A' → d ¹ A'	σ _{Re-H} - 5d _{xz} → π _{DAB} * (0.64) 5d _{xz} + σ _{Re-H} → π _{DAB} * (0.59) SBLCT/MLCT (f = 0.12)	31 340

the visible spectroscopic and photochemical properties. Indeed, for the hydride complex, the two low-lying singlet excited states are purely MLCT in character, and their associated potentials are quasi-bound with respect to the Mn-H elongation and weakly bound with respect to the axial carbonyl departure.¹³ Nonproductive decay from the low-lying MLCT states or/and carbonyl dissociation will more likely be the excited-state behavior of this model hydride complex. A more complex mechanism is expected for the alkyl complexes since both metal-R bond homolysis and carbonyl dissociation may be efficient in the same experimental conditions. In practice, a hydride complex could not yet be synthesized and studied. However, the photochemical behavior of the Mn(R)(CO)₃(Pr-DAB) (R = methyl, benzyl) complexes is in line with the predictions from the above calculations.⁸ The methyl complex shows only release of CO, whereas the benzyl complex undergoes an efficient homolysis of the Mn-benzyl bond and a very ineffective CO dissociation.

Re(H)(CO)₃(H-DAB) Excited States. The CASSCF/MR-CCI excitation energies to the low-lying singlet and "pseudotriplet" states of Re(H)(CO)₃(H-DAB) are reported in Table 2.

The substitution of the first-row transition metal by a rhenium atom has two important consequences for the spectrum of the low-lying excited states in M(H)(CO)₃(H-DAB) (Tables 1 and 2): (i) a lowering of the excitation energies; (ii) a significant mixing between the so-called MLCT and SBLCT states corresponding to d_M → π*_{DAB} and σ_{M-H} → π*_{DAB} excitations, respectively.

The decrease in energy of both MLCT and SBLCT transitions on going from the manganese to the rhenium complex is a direct consequence of the relativistic destabilization of the d shells and of the stabilizing interaction between the π*_{DAB} vacant orbital and the 6p_z of the heavy atom. Like in the manganese complex, we observe a reverse order of the two low-lying singlet and triplet states. The transition to the lowest singlet state, calculated at 15 250 cm⁻¹, corresponds to the nearly pure 5d_{x²-y²} → π*_{DAB} MLCT excitation and has a negligible oscillator strength. This transition should only contribute weakly to the absorption spectrum. The transition to the next singlet state, calculated at 21 720 cm⁻¹ with an oscillator strength of 0.32, matches well with the intense absorption band around 20 000 cm⁻¹ of this class of rhenium complexes.¹⁷ The SBLCT/MLCT singlet state, calculated at 31 340 cm⁻¹ with an oscillator strength of 0.12, should be responsible for a less intense band in the UV energy domain. The calculated excitation energies to the lowest triplet states of Re(H)(CO)₃(H-DAB) have no

quantitative significance. An appreciable spin-orbit splitting of the triplet states is expected for this third-row transition metal complex. However, these preliminary results, which have to be improved by the introduction of the spin-orbit coupling effects at the CCI level,³⁸ indicate the same trends for the singlet and for the triplet states. The mixed MLCT/SBLCT character of the transition to the singlet state, contributing mainly to the visible band, could lead to substantial distortions of the shapes of the associated potentials. This may have large consequences on the visible spectroscopic and photochemical properties of the model complex with respect to those of the Mn compound discussed above. Contrary to the lowest optically accessible excited state of the Re complex, that of the corresponding Mn compound is purely MLCT in character (vide supra). Up to now, the attempts to synthesize any M(H)(CO)₃(R-DAB) (M = Mn, Re) complex failed, and their photochemical behavior can therefore not be compared with the results from the present calculations on the model compounds M(H)(CO)₃(H-DAB) (M = Mn, Re). However, a comparison of the behavior of the two complexes M(Me)(CO)₃(Pr-DAB) (M = Mn, Re) shows that the replacement of Mn by Re has a pronounced effect on the photochemistry. The Mn complex loses CO,⁸ whereas the corresponding Re complex undergoes homolysis of the Re-Me bond with a low quantum yield.⁷ This different behavior points to an increase of SBLCT character of the lowest excited state in the case of the Re complex. For the corresponding benzyl complexes M(Bz)(CO)₃(Pr-DAB) (M = Mn, Re) the photochemistry is already very much the same, both complexes undergoing an efficient homolysis of the metal-benzyl bond.^{3,7,8}

4. Conclusion

On the basis of accurate CASSCF/MR-CCI calculations (either in the all-electron scheme for Mn(R)(CO)₃(H-DAB) or in the effective core potential approximation for Re(H)(CO)₃(H-DAB)), it has been shown that the three-center interaction between the group R (R = H, Me, or Et), the metal center (M = Mn or Re), and the π* acceptor H-DAB ligand controls entirely the photochemical and photophysical properties of this class of model complexes. The balance between the strength of the metal-R bond, the basicity of the R group, and the polarized character of the bond, for a given metal center and a given π* acceptor ligand, determines the main features of the lowest part of the electronic spectrum. According to experimental findings, variation of the metal center, of R, or of the α-diimine group strongly influences the behavior of the real complexes M(R)(CO)₃(α-diimine) upon irradiation in the visible. Until now, the unconventional photophysical and photochemical properties of these complexes could not easily be rationalized. This is probably due to the extreme sensitivity of the electronic response to the metal center environment. Increasing the delocalization of the electronic density through these three centers (M, R, α-diimine), the character of the low-lying excited states is fundamentally modified from purely MLCT to mixed MLCT/SBLCT. In the examples reported in the present work, this is achieved either by substitution of the hydrogen by an alkyl group or by the replacement of a first-row transition metal center by a third-row metal atom. A detailed knowledge of the potential energy surfaces associated with these low-lying excited states is necessary to obtain more information concerning the shape of the absorption spectra and the photodissociation dynamics. This theoretical work has to be driven in close connection with fast time-resolved spectroscopy and photochemical experiments.

(38) Ribbing, C. Daniel, C. *J. Chem. Phys.* **1994**, *100*, 6591.

Acknowledgment. The authors are grateful to Prof. M. Dolg, Dr. J. L. Heully, and Dr. M. Péliissier for their collaboration in the handling of the effective core potentials in Molcas 3.0. Generous financial support from the European Community and from the CNRS for the COST D4/00194/project entitled "Design and preparation of new molecular systems with unconventional electrical, optical and magnetic properties" is gratefully acknowledged. M.P.W. acknowledges The Netherlands Foundation

for Chemical Research (SON) for a visiting grant. The calculations have been carried out on the C98 computer of the IDRIS (Orsay, France) through a grant of computer time from the Conseil Scientifique and on the workstations of the Laboratoire de Chimie Quantique (Strasbourg).

IC9802552